Available online at www.sciencedirect.com
ScienceDirect
Journal of Power Sources 159 (2006) 752–757
JOURNAL OF POWER SOURCES
www.elsevier.com/locate/jpowsour

# Zn/gelled 6 M KOH/$O_2$ zinc–air battery

A.A. Mohamad *

*School of Materials and Mineral Resources Engineering, Universiti Sains Malaysia, 14300 Nibong Tebal, Penang, Malaysia*

Received 24 August 2005; received in revised form 30 September 2005; accepted 3 October 2005
Available online 3 February 2006

**Abstract**

The gel electrolyte for the zinc–air cell was prepared by mixing hydroponics gel with a 6 M potassium hydroxide aqueous solution. The self-discharge of cells was characterized by measuring the open-circuit voltage. The effect of a discharge rate of 50 mA constant current on cell voltage and plateau hour, as well as the voltage–current and current density–power density were measured and analysed. The electrode degradation after discharge cycling was characterized by structural and surface methods. The oxidation of the electrode surface further blocked the utilization of the Zn anode and was identified as a cause for the failure of the cell.


*Keywords:* Zinc–air battery; Polymer gel electrolyte; Air–electrode; Potassium hydroxide; Oxidation

## 1. Introduction

Gel electrolytes are emerging as useful materials for technological applications [1]. The conductivity of the gel electrolytes can be expected to be very close to the corresponding liquid electrolyte, which is generally greater than $10^{-3}$ S cm$^{-1}$ [2], and this has led to their application in many electrochemical solid state ionic devices such as high-energy density batteries, fuel cells, sensors and electrochemical display devices. Although the primary zinc–air (Zn–air) battery has been commercialized in the 1920s [3], there were only a few reports on polymer-based electrolyte Zn–air batteries. For example, the hydroponics gel [4–6], epichlorohydrin-ethylene oxide [P(ECH-*co*-EO)] [7] and polyvinyl alcohol (PVA)–polyethylene oxide (PEO)–glass-fibre-mat [8,9] doped with potassium hydroxide (KOH) have been used as the electrolyte component in a Zn–air battery.

The discharge reactions for the Zn–air rechargeable battery using Zn as the anode, and an air–electrode as the cathode and KOH as the electrolyte solution are as follows [10,11]:

- At the positive (cathode) electrode:

$$O_2 + 2H_2O + 4e^- \rightarrow 4OH^-, \quad E^0 = 0.40\,V$$

- At the negative (anode) electrode:

$$2Zn \rightarrow 2Zn^{2+} + 4e^-,$$

$$2Zn^{2+} + 4OH^- \rightarrow 2Zn(OH)_2, \quad E^0 = 1.25\,V$$

$$2Zn(OH)_2 \rightarrow 2ZnO + 2H_2O$$

- Overall cell reaction:

$$2Zn + O_2 \rightarrow 2ZnO, \quad E^0 = 1.65\,V$$

The hydroponics gel–KOH electrolyte and planar Zn anode has been studied by Othman et al. [4], using a low KOH concentration of 2.8 M. However, Iwakura et al. [12] reported that the highest conductivity in polymer gel–KOH mixtures are achieved at 6 M KOH concentration. In this paper, 6 M KOH was gelled as a hydroponics gel and used to obtain a relatively improved cell performance. The cells were tested for self-discharge by measuring the open-circuit voltage (OCV) and discharge characteristics. The anode and cathode electrode degradation after cycling discharge were characterized by structural and morphological analysis.

* Tel.: +604 599 6118; fax: +604 594 1011.
*E-mail address:* azmin@eng.usm.my.

0378-7753/$ – see front matter © 2005 Elsevier B.V. All rights reserved.
doi:10.1016/j.jpowsour.2005.10.110

## 2. Experimental

### 2.1. Cell fabrication

Since this paper is a comparative work, all the materials used and the design of the cell are equivalent to the work by Othman et al. [4]. A circular-shaped 99.98% purity Zn plate (LabChem, Malaysia) with an active area of 12.6 $cm^2$, weight 4.0 g and thickness 0.3 mm and a small portion left for the negative terminal, was used as the anode. The commercial fibre-carbon–$MnO_x$ air–electrode (ECT, UK) was used as the cathode. The air–electrode consists of two catalyst layers bonded to each side of a nickel mesh. A Teflon layer was used to prevent water leaking and at the same time allowed transfer of air. The air–cathode sheet was cut into a circular shape (active area 12.6 $cm^2$, weight 0.9 g and thickness 0.5 mm) with a small portion left for the positive terminal.

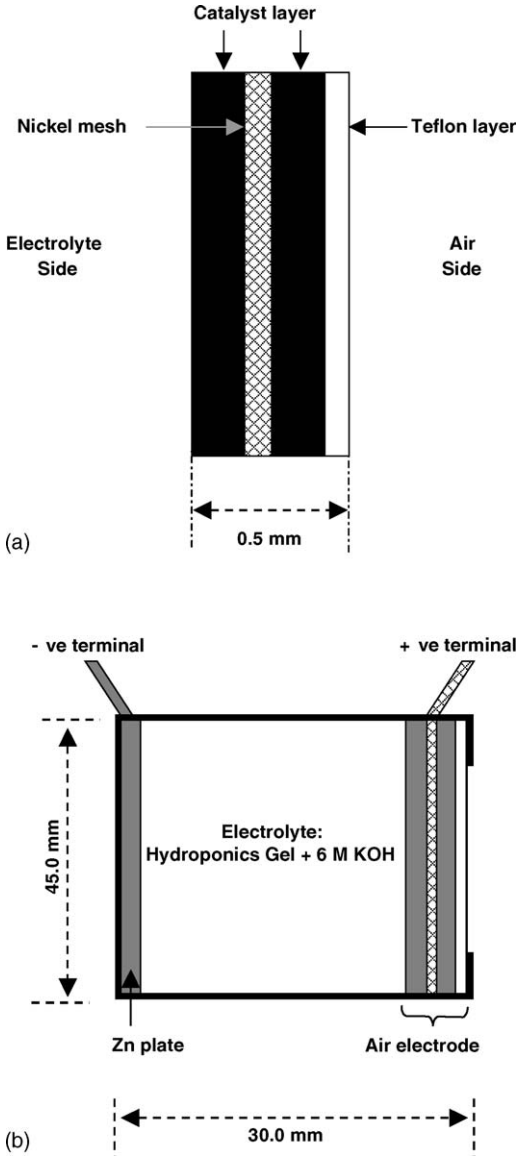


Fig. 1. Cross-sectional view of: (a) laminated cross-section air–electrode layers and (b) Zn–air cell assembly from its components.

A cylindrical plastic casing with the dimensions of 30 mm length and 45 mm diameter was filled with 2.4 g granular form hydroponics gel (YMWoo Corp, Malaysia). The electrolyte solution (6 M KOH and volume 35 ml) was injected into the cell casing. After 30 min, the gel expanded into a loosely bounded, elastic jelly granule. The entire cell with the electrolyte is 70.75 g weight. Fig. 1 shows a schematic design of the Zn/gelled 6 M $KOH/O_2$ cell.

### 2.2. Cell characterization

The OCV, discharge and voltage–current, and power density–current density characteristics of the cell were measured using a BAS LG-50 galvanostat system. The OCV was measured for the cell stored at an open-circuit condition for 24 h. The cells were discharged using a constant current of 50 mA. Three cells have been used in order to plot variations. Cell characterizations were performed at room temperature (25 °C). After the cell has been discharged, the anode and cathode were dismantled, cleaned and dried in a desiccator. The electrodes were characterized by using an X-ray diffraction (XRD, Siemens D5000), scanning electron microscopy (SEM, Leica S440) and an optical microscope (Olympus BX51M). The XRD results obtained were compared to the American Society for Testing and Materials (ASTM) X-ray data file. The cross-section of Zn plate was prepared by mounted in acrylic resin, then polished with SiC paper and diamond paste.

## 3. Results and discussion

### 3.1. Cell characterization

Fig. 2 shows the OCV characteristic of the Zn/gelled 6 M $KOH/O_2$ cell. The OCV of the cells remained steady at $1.48 \pm 0.03$ V during 24 h of storage. Most practical cells have an OCV range between 1.42 and 1.52 V [11]. The OCV value obtained in the present study was in accordance with the value reported by Othman et al. [4] using Zn/gelled 2.8 M $KOH/O_2$. It can be observed that the OCV value was not influenced by the KOH concentration.

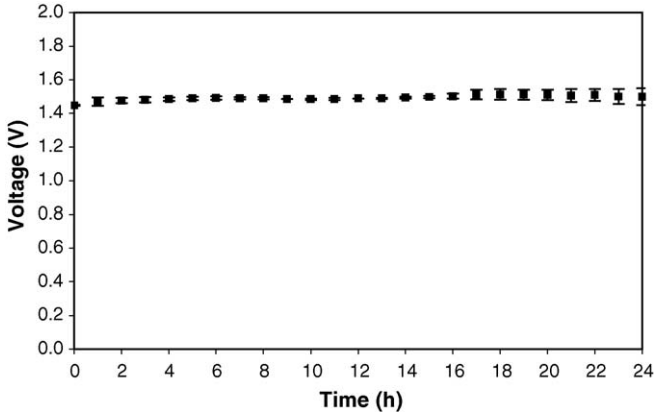


Fig. 2. The open circuit voltage measurement of Zn/gelled 6 M $KOH/O_2$ for 24 h.

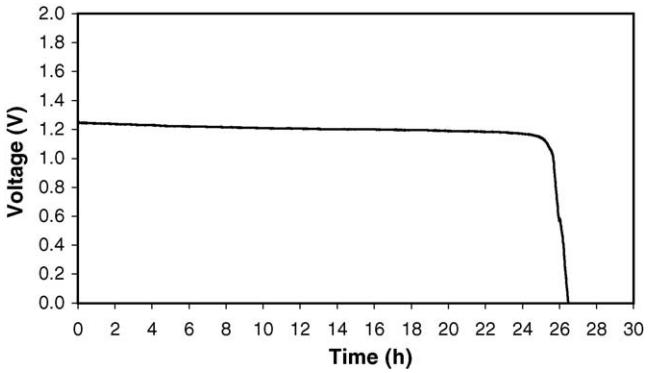


Fig. 3. Discharge plot using a constant current at 50 mA.

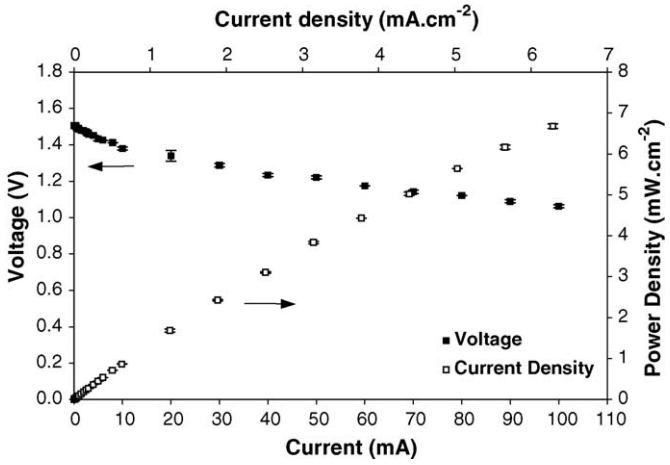


Fig. 4. The plot of operating voltage–current and power density–current density for Zn/gelled 6 M KOH/$O_2$ cells.

Fig. 3 shows the discharge characteristics at a constant current of 50 mA, which gave a flat discharge plateau at 1.20 V. It shows that the discharge was sustained for 26.3 h. The cell showed a longer discharge time compared to Othman et al. [4].

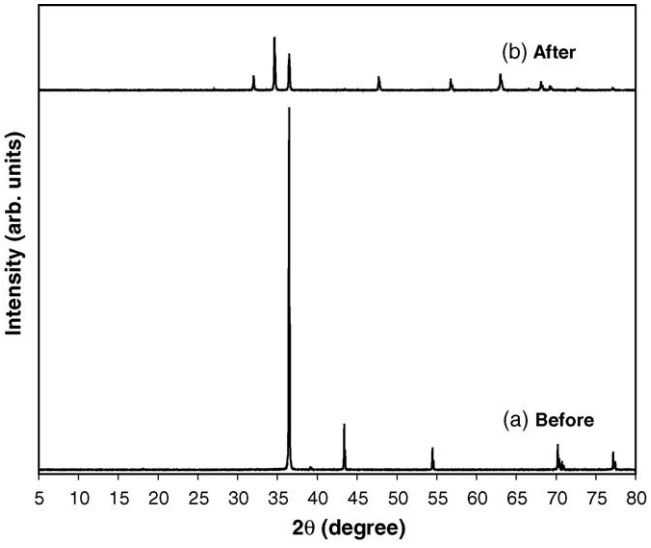


Fig. 5. X-ray diffractiongram of Zn anode plate electrode: (a) before discharge and (b) after complete discharge at 50 mA.

Current drains ranging from 2 μA to 100 mA were used to plot the voltage–current and power density–current density curves as depicted in Fig. 4. The average of each cell's voltage was monitored for each current drain after 10 s of operation. The voltage dropped from 1.51 to 1.06 V during the increased current that is from 2 μA to 100 mA. This could be due to the parasitic corrosion reaction that had degraded the efficiency of the anode. The plot of operating voltage–current and current density–power density of the cell are in good agreement with the reported gel-type [4] and aqueous-type electrolytes [13,14].

### 3.2. Electrode characterization

The comparative XRD patterns of the anode material before and after the discharge are illustrated in Fig. 5. The XRD pattern of the pure Zn anode agrees with ASTM (4-083) at $2\theta = 36.5^\circ$, $39.2^\circ$, $43.4^\circ$ and $54.5^\circ$. After the discharge, the surface of the original anode transformed to a rough surface and formed white spots. These white spots could possibly be ZnO. In order to

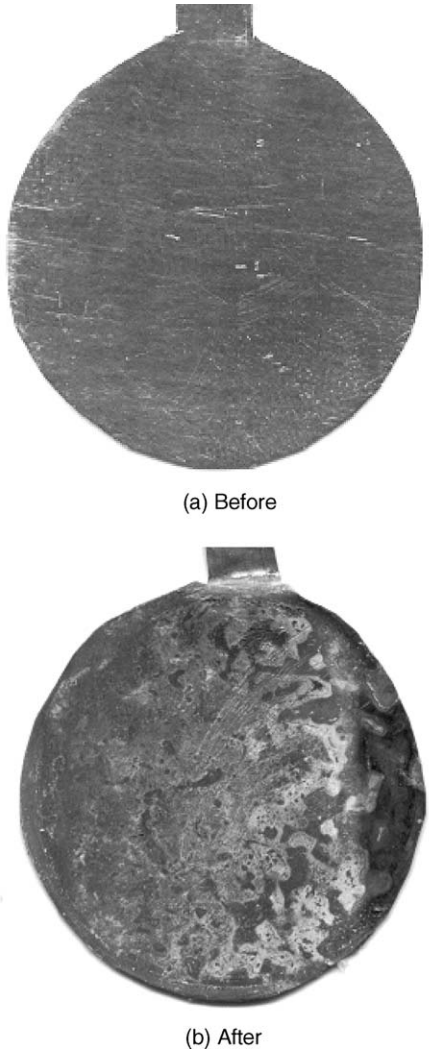


Fig. 6. Circular Zn anode plates: (a) before discharge and (b) after complete discharge at 50 mA.

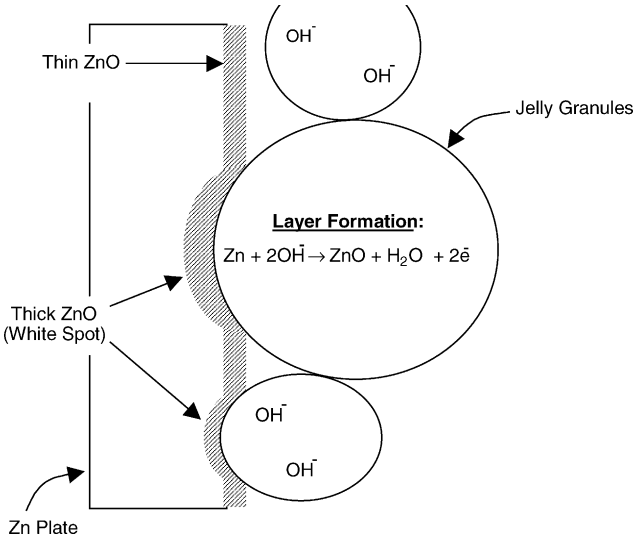


Fig. 7. Schematic cross-section of reaction between Zn plate and $OH^-$ inside jelly granules.

confirm these white spots, XRD was performed. The observed peaks matched quite well with the values of ZnO when compared with ASTM (5-0664) at $2\theta = 31.2°$, 33.9°, 35.8°, 47.0°, 56.2°, 62.4° and 67.58°. This confirms that based on the XRD data, the failure of the anode is due to the oxidation of Zn which formed a ZnO layer. The degradation of Zn electrode due to the formation of ZnO has been studied by many researchers particularly in aqueous alkaline solutions [15–21]. Generally, during the discharge, Zn is oxidized to form solid zinc oxide or was transformed into a soluble complex zincate ion in the presence of excess alkaline. The overall reactions are normally considered to be as follows [14,22–24]:

$$Zn + 2OH^- \rightarrow ZnO + H_2O + 2e^- \quad \text{(layer formation)},$$

$$Zn + 4OH^- \rightarrow Zn(OH)_4{}^{2-} + 2e^- \quad \text{(dissolution)}$$

Fig. 6 shows the surface of Zn plate before and after the discharge. As mentioned earlier, the white spots are ZnO. Actually, these areas are where the reaction between the electrolytes in the jelly granules and Zn plate took place. The white spots were observed to be thicker compared with other areas. The oxidation of other areas is due to the reaction with excess liquid electrolyte and Zn plate. Fig. 7 shows the schematic contact and reaction between the jelly granules and Zn plate that produces the white spots or oxide layer. It could also be observed that the shape of the circular Zn plate did not show any change after the discharge, which indicates that the gel electrolytes did not cause any change in the shape. In liquid electrolyte cells, the electrode

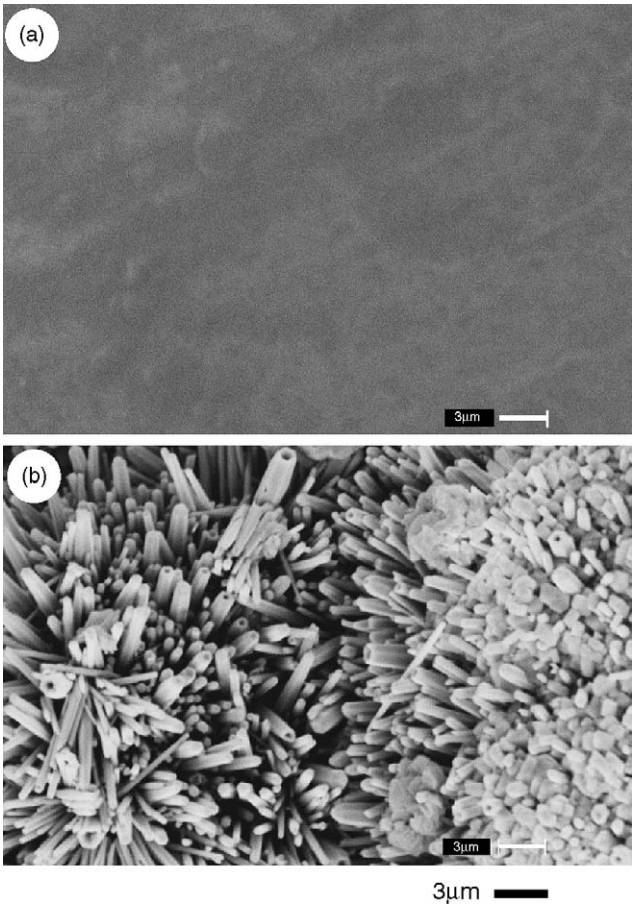


Fig. 8. Scanning electron micrograph of zinc anode plates: (a) before discharge and (b) after complete discharge at 50 mA.

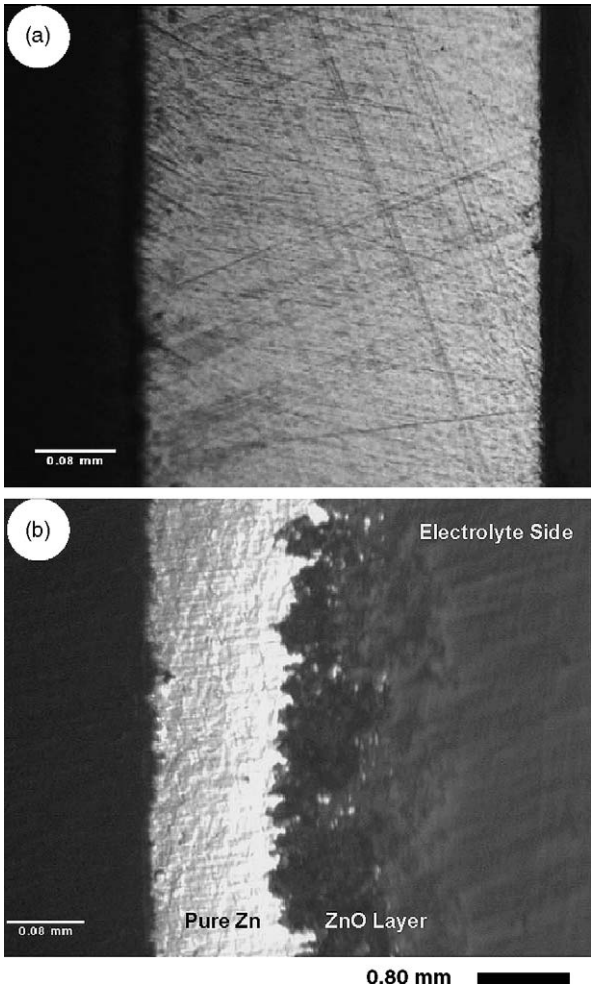


Fig. 9. Optical micrograph cross-sections of zinc anode plates: (a) before discharge and (b) after complete discharge at 50 mA.

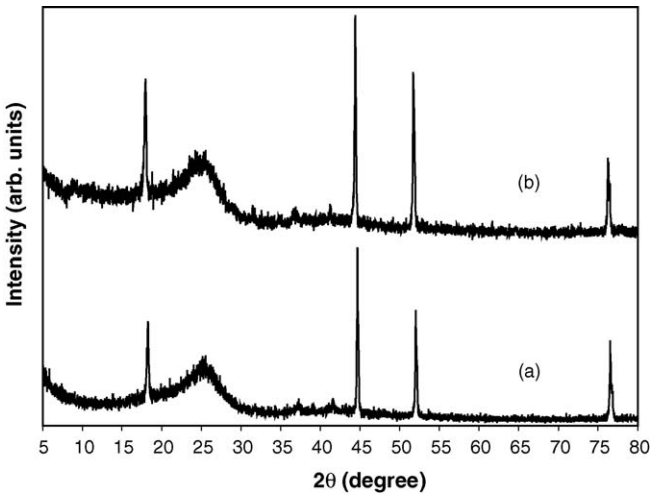


Fig. 10. X-ray diffractiograms of air–electrode: (a) before discharge and (b) after complete discharge at 50 mA.

generally change shape due to the dissolution of zinc into the electrolyte [25–29]. The SEM micrographs of the zinc anode before and after the discharge are depicted in Fig. 8. The anode surface was covered by the rod-like structures of ZnO. This ZnO structure was quite similar to the structure observed by Othman et al. [4] and Lao et al. [30].

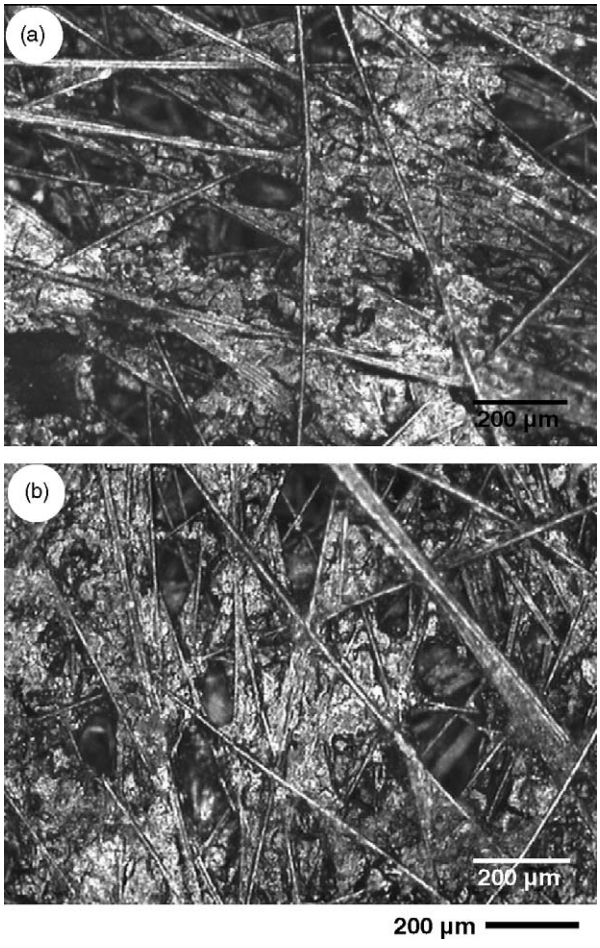


Fig. 11. Optical micrographs of air–electrode surface: (a) before discharge and (b) after complete discharge at 50 mA.

Fig. 9 shows the cross-section of Zn anodes before and after the discharge at 50 mA. It can be observed that about 50% of the electrolyte side of the Zn anode was used in the discharge reaction. This finding also correlates well with the discharge time (Fig. 3). Based on the calculation, 50% of 4.0 g weight of Zn plate is equal to 2.0 g, gave the specific capacity of the cell that is 657.5 mAh $g^{-1}$. The result is reasonable compared to the theoretical value of 820 mAh $g^{-1}$ [31,32]. However, the result showed that the capacity is lower than expected from the 4.0 g Zn plate, which is 3.28 Ah $g^{-1}$ ($4 \times 0.82$ Ah $g^{-1}$). Since the Zn anode used in this cell is in the compact planar form, thus the Zn is not fully utilized for the discharge reaction, which is why the capacity is lower when compared to the theoretical value.

The XRD study of the air–electrode components is shown in Fig. 10. The XRD measurement was taken for each component, i.e. fibrous carbon–$MnO_x$, nickel mesh and all air–electrode components. The peaks detected at $2\theta = 44.6^\circ$, $52.0^\circ$ and $77.0^\circ$ are assigned to the nickel mesh, whereas the $2\theta = 18.5^\circ$ peak is attributed to the fibrous carbon–$MnO_x$ material. These peaks remained unchanged after a complete discharge. The optical micrograph after the discharge showed that on the electrolyte side, the catalyst and fibrous material covered the surface (Fig. 11). The surface of the air–electrode remained unchanged after the discharge.

## 4. Conclusion

The gelled 6 M KOH electrolytes used in the present work has improved cell specific capacity to 657.5 mAh $g^{-1}$ (789 W $kg^{-1}$) compared to using 2.8 M KOH, as was reported in previous work by Othman et al. The OCV was not influenced by the concentration of KOH. Based on the XRD observation and supported by morphology analysis, the failure of the battery could be attributed to the degradation of the Zn anode. The formation of a ZnO layer hampers continuous reaction with $OH^-$ and the discharge of cell ceased. The air–electrode and gelled electrolytes did not show any degradation.

## Acknowledgements

The author would like to gratefully acknowledge Universiti Sains Malaysia for the Short Term Grant 2005/07 and experimental facilities from Prof. A.K. Arof (University Malaya).

## References

[1] S. Chandra, S.S. Sekhon, R. Srivastava, N. Arora, Solid State Ionics 154/155 (2002) 609.
[2] S.A. Agnihotry, K.V. Pradeep, S.S. Sekhon, Electrochim. Acta 44 (1999) 3121.
[3] E.A. Schumacher, Zinc:Oxygen cells with alkaline electrolytes, in: G.W. Heise, N.C. Cohoon (Eds.), Primary Battery, vol. 1, John Wiley & Sons Inc., 1994, p. 265.
[4] R. Othman, W.J. Basirun, A.H. Yahaya, A.K. Arof, J. Power Sources 103 (2001) 34.

[5] R. Othman, A.H. Yahaya, A.K. Arof, J. N. Mater. Electrochem. Syst. 5 (2002) 177.
[6] R. Othman, A.H. Yahaya, A.K. Arof, J. Appl. Electrochem. 32 (2002) 1347.
[7] N. Vassal, E. Salmon, J.-F. Fauvarque, Electrochim. Acta 45 (2000) 1527.
[8] C.C. Yang, S.J. Lin, S.T. Hsu, J. Power Sources 122 (2003) 210.
[9] C.C. Yang, S.J. Lin, J. Power Sources 112 (2002) 497.
[10] S.F. Bender, J.W. Cretzmeyer, T.F. Reise, Zinc/air cells, in: D. Linden (Ed.), Handbook of Batteries, 2nd ed., McGraw-Hill, New York, 1994, p. 131.
[11] T.R. Crompton, Metal air batteries, in: Batteries Reference Book, 3rd ed., Newnes, 2000, pp. 12/1 and 26/1.
[12] C. Iwakura, S. Nohara, N. Furukawa, H. Inoue, Solid State Ionics 148 (2002) 487.
[13] S. Muller, F. Holzer, O. Haas, C. Schlatter, C. Comninellis, Chimia 49 (1995) 27.
[14] S. Muller, F. Holzer, O. Haas, J. Appl. Electrochem. 28 (1998) 895.
[15] S.S. Abd El Rehim, S.M. Abd El Wahad, E.E. Fouad, H.H. Hassan, Mater. Corros. 46 (1995) 633.
[16] S.S. Abd El Rehim, A.A. El Basosi, M.M. Osman, J. Electroanal. Chem. 348 (1993) 99.
[17] T.C. Chang, G.J. Prentice, J. Electrochem. Soc. 131 (1984) 1465.
[18] T.C. Chang, G.J. Prentice, J. Electrochem. Soc. 136 (1989) 3398.
[19] G.J. Prentice, T.C. Chang, X. Shan, J. Electrochem. Soc. 138 (1991) 890.
[20] P.L. Cabot, M. Corter, F.A. Centellas, J.A. Garrido, J. Electroanal. Chem. 201 (1986) 85.
[21] P.L. Cabot, M. Corter, F.A. Centellas, J.A. Garrido, Electrochim. Acta 31 (1987) 1321.
[22] J.W. Cretzmeyer, H.R. Espig, R.S. Melros, Commercial Zn–air batteries, in: D.H. Collins (Ed.), Power Sources 6: Proceedings of the 10th International Symposium on Research and Development in Non-mechanical Electrical Power Sources 1976, Academic Press Inc., London, 1977, p. 269.
[23] M. Ghaemi, R. Amrollahi, F. Ataherian, M.Z. Kassaee, J. Power Sources 117 (2003) 233.
[24] A.L. Rudd, C.B. Breslin, Electrochim. Acta 45 (2000) 1571.
[25] S. Guinot, E. Salmon, J.F. Penneau, J.F. Fauvarque, Electrochim. Acta 43 (1998) 1163.
[26] F.R. McLarnon, E.J. Cairns, J. Electrochem. Soc. 138 (1991) 645.
[27] T.C. Adler, F.R. McLarnon, E.J. Cairns, J. Electrochem. Soc. 140 (1993) 289.
[28] J. Jorne, T.C. Adler, E.J. Cairns, J. Electrochem. Soc. 142 (1995) 771.
[29] M. Klein, F. McLarnon, Nickel–zinc batteries, in: D. Linden (Ed.), Handbook of Batteries, 2nd ed., McGraw-Hill, New York, 1994, p. 29.1.
[30] J.Y. Lao, J.G. Wen, Z.F. Ren, Nano Lett. 2 (2002) 1287.
[31] A.J. Appleby, M. Jacquier, J. Power Sources 1 (1976–1977) 17.
[32] D.A.J. Rand, J. Power Sources 4 (1979) 101.